DOI: 10.1002/ejic.200801038

Kinetics of Bis(*p*-nitrophenyl)phosphate (BNPP) Hydrolysis Reactions with Trivalent Lanthanide Complexes of *N*-Hydroxyethyl(ethylenediamine)-*N*,*N*′,*N*′-triacetate (HEDTA)[‡]

C. Allen Chang,*[a] Yu-Ping Chen,[a] and Chih-Hsiang Hsiao[a]

Keywords: Lanthanides / Hydrolysis / Kinetics / Macrocyclic complexes / Phosphodiesters / Reaction mechanisms

Kinetic studies of hydrolysis reactions of BNPP [sodium bis(*p*-nitrophenyl)phosphate] with trivalent lanthanide (Ln^{3+}) complexes of HEDTA [HEDTA = *N*-hydroxyethyl(ethylenediamine)-*N*,*N*′,*N*′-triacetate] were performed at pH 6.96–11.34 and 25 °C by a spectrophotometric method and by HPLC analysis. The reaction rates increase with increasing atomic number of lanthanide and solution pH from PrHEDTA to EuHEDTA and then decrease for heavier LnHEDTA complexes. Plots of pseudo-first-order rate constants (k_{obs}) vs. pH could be fitted to the equation $k_{obs} = k_{LnL(OH)}[LnL]_T/\{1+\exp[-2.303(pH-pK_h)]\}$, where $k_{LnL(OH)}$ is the rate constant for the reaction of $LnHEDTA(OH)^-$ with BNPP, K_h is the hydrolysis constant of LnHEDTA, and $[LnL]_T$ is the total concentration of LnHEDTA. The pK_h values obtained by the kinetic method are in the range 8.2–10.3 and are similar to those measured by potentiometric methods. At $[LnL]_T$ = 10–70 mM and pH 10.5, most of the observed pseudo-first-order rate constants could be fitted to a simple saturation kinetic model, $k_{obs} = k_1K[LnHEDTA(OH)^-]/\{1 + K[LnHEDTA(OH)^-]\}$, where K is the equilibrium constant for the formation for $LnHEDTA(OH)^-BNPP$ and is in the range 2–147 M^{-1}. The k_1 values are in the range 1.12×10^{-5}–2.71×10^{-3} s^{-1}. The k_{obs} data for TbHEDTA and HoHEDTA were fitted to a quadratic equation. It was observed that the dinuclear species are more reactive. ESI mass spectrometry confirmed that the reaction between BNPP and EuHEDTA is a simple hydrolysis but not a transesterification, presumably because the three inner-sphere coordinated water molecules are far away from the coordinated hydroxyethyl group. Hydrolysis is likely to occur by proton transfer from one inner-sphere coordinated water molecule to the deprotonated ethyl oxide group followed by nucleophilic attack of the resulting hydroxide ion on the bonded BNPP anion.

Introduction

Trivalent lanthanide cations (Ln^{3+}) are good Lewis acids and have been demonstrated to be potential effective cleavage agents for DNA, RNA, and phosphodiester compounds.[1–4] Because of their complicated hydrolytic properties leading to various insoluble hydroxido- and/or oxido-bridged species, applications of lanthanide ions at physiological or higher pH are quite limited. Instead, suitable ligands are designed and used to form trivalent lanthanide complexes to control lanthanide-promoted hydrolysis for more specific usage.[5–14]

We have been interested in the use of macrocyclic lanthanide complexes as artificial nucleases and ribonucleases, because these complexes are thermodynamically more stable and kinetically inert. Previously we reported the coordination properties of $LnDO2A^+$ complexes (DO2A = 1,7-dicarboxymethyl-1,4,7,10-tetraazacyclododecane)[15] and their promotion of BNPP [sodium bis(*p*-nitrophenyl)phosphate] phosphodiester bond hydrolysis.[16] We have preliminarily evaluated the effects of pH, metal ionic radii, number of coordinated water molecules, charges and concentrations of a number of trivalent lanthanide complexes on the rates of BNPP hydrolysis. However, $LnDO2A^+$ complexes seem to form various oligomeric species at high pH with different rates, making it difficult and complicated to carry out appropriate thermodynamic and kinetic studies and to interpret the experimental results.[17] A separate study on $Ln(NO2A)^+$ complexes with 3–4 inner-sphere coordinated water molecules (Ln = Eu^{III} and Yb^{III}, and NO2A = 1,7-dicarboxymethyl-1,4,7-triazacyclononane) revealed much faster oligomerization processes leading to less efficient BNPP hydrolysis.[17] Thus, the number and spatial arrangements of the inner-sphere coordinated water molecules are potentially important to effect the BNPP hydrolysis and oligomerization processes.

To understand these problems better and for purposes of comparison, we performed kinetic studies on the BNPP hydrolysis reaction promoted by LnHEDTA complexes,

[‡] Macrocyclic Lanthanide Complexes as Artificial Nucleases and Ribonucleases, 2. Part 1: Ref.[16]

[a] Department of Biological Science and Technology
National Chiao Tung University
75 Po-Ai Street, Hsinchu, Taiwan 30039, Republic of China
Fax: +886-3-5729288
E-mail: changca@cc.nctu.edu.tw

Supporting information for this article is available on the WWW under http://www.eurjic.org or from the author.

where HEDTA is a linear ligand [*N*-Hydroxyethyl(ethylenediamine)-*N*,*N*′,*N*′-triacetate]. Ln^{III}HEDTA complexes are neutral and do not form hydroxido- or oxido-bridged oligomers at pH values below ca. 11.5, except for TbHEDTA. In addition to obtaining important fundamental parameters including the binding constants of BNPP with the lanthanide complexes and the rate constants of BNPP hydrolysis in the presence of Ln^{III}HEDTA complexes under simpler, non-aggregate-forming conditions, it is of interest to examine in what manner the coordinated *N*-hydroxy group participates in the BNPP hydrolysis reaction. Previously, Baker et. al reported that $Eu(THED)^{3+}$ [THED = 1,4,7,10-tetrakis(2-hydroxyethyl)-1,4,7,10-tetraazacyclododecane] cleaved the 5′ cap structure of mRNA and resulted in the formation of THED-phosphate transesterification adducts.[8] In our present study, we found that the reaction of BNPP with EuHEDTA at pH 10.5 and 25 °C is a simple hydrolysis reaction in which the cleaved nitrophenylphosphate (NPP) anion from BNPP does not form an ester bond with the coordinated *N*-hydroxyethyl group of LnHEDTA. This paper reports the results.

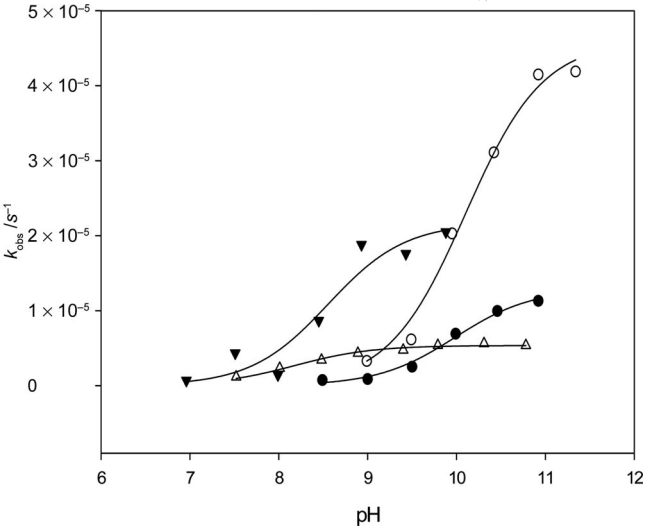

Figure 1. Plots of selected observed BNPP hydrolysis reaction rate constants vs. solution pH in the presence of 10 mM LnHEDTA. [BNPP] = 0.1 mM, [buffer] = 100 mM, μ = 0.1 M at 25.0 ± 0.1 °C. Solid lines are the best least-squares fits to Equation (1); Pr (●), Eu (○), Ho (▼), Yb (Δ).

Results and Discussion

Choice of Lanthanide–HEDTA Complexes for the Study

All trivalent lanthanide–HEDTA complexes were chosen for the present study except lanthanum and cerium. The lanthanum(III)–HEDTA complex has very limited solubility[18] and the cerium(III)–HEDTA complex is prone to air oxidation and makes the BNPP hydrolysis more complicated.[6,19–20] The LnHEDTA complexes chosen are neutral and very stable in the pH range and concentrations used in this study.

$$LnHEDTA <=> LnHEDTA(OH)^- + H^+ \qquad K_h$$

$$LnHEDTA(OH)^- + BNPP \rightarrow Products \qquad k_{LnL(OH)}$$

$$Rate = k_{obs}[BNPP] = k_{LnL(OH)}[LnL(OH)][BNPP]$$

$$k_{obs} = k_{LnL(OH)}[LnL(OH)]$$

$$K_h = [LnL(OH)][H^+]/[LnL(H_2O)]$$

$$[LnL]_T = [LnL(H_2O)] + [LnL(OH)]$$

$$k_{obs} = k_{LnL(OH)}K_h[LnL]_T/(K_h + [H^+]) = k_{LnL(OH)}[LnL]_T/(1 + [H^+]/K_h)$$

$$\text{or } k_{obs} = k_{LnL(OH)}[LnL]_T/(1 + \exp\{-2.303(pH - pK_h)\}) \qquad (1)$$

Scheme 1.

Effects of pH on the Reactions of BNPP with LnHEDTA

Table S1 (Supporting Information) lists the observed BNPP hydrolysis reaction rate constants (k_{obs}) calculated from the measured initial rate data at various solution pH values in the presence of 10 mM LnHEDTA. Figure 1 shows selected k_{obs} vs. pH plots from the data in Table S1. It is observed that the k_{obs} values increase in a sigmoid fashion as the solution pH increases, and they are much greater than those of the simple OH^- catalyzed hydrolysis reactions where $k_{obs} = 2.3 \times 10^{-5}[OH^-]\ s^{-1}$.[16] This indicates that the active LnHEDTA species for the BNPP hydrolysis reaction is the deprotonated $Ln(HEDTA)(OH)^-$. The deprotonation very likely occurs at the coordinated hydroxyethyl functional group (vide infra).

By fitting the k_{obs} vs. pH data to Equation (1), obtained by the derivation shown in Scheme 1, we calculated the $k_{LnL(OH)}$ and pK_h values for all LnHEDTA complexes studied, and the results are listed in Table 1. Also listed are the pK_h values for LnHEDTA complexes and Ln^{3+} ions determined by potentiometric methods.

Table 1. Fitted pK_h and $k_{LnL(OH)}$ values for BNPP hydrolysis reactions in the presence of 10 mM LnHEDTA, [buffer] = 100 mM, [BNPP] = 0.10 mM, μ = 0.1 M at 25.0 ± 0.1 °C.

	$k_{LnL(OH)}$ /$M^{-1}s^{-1}$	pK_h	R^2	pK_h[a]	$pK_h(Ln^{3+})$[b]
PrHEDTA	$1.29(\pm0.07)\times10^{-3}$	9.99 ± 0.07	0.9965	10.08	8.63
NdHEDTA	$1.37(\pm0.13)\times10^{-3}$	10.15 ± 0.13	0.9758	10.18	8.51
SmHEDTA	$4.70(\pm0.28)\times10^{-3}$	9.99 ± 0.08	0.9868	10.07	8.42
EuHEDTA	$4.60(\pm0.18)\times10^{-3}$	10.10 ± 0.07	0.9927	9.74	8.39
GdHEDTA	$5.15(\pm0.34)\times10^{-3}$	10.29 ± 0.08	0.9921	9.79	8.43
TbHEDTA	$2.48(\pm0.09)\times10^{-3}$	9.07 ± 0.08	0.9873	9.25	8.24
DyHEDTA	$8.80(\pm0.03)\times10^{-4}$	9.07 ± 0.07	0.9899	8.89	8.18
HoHEDTA	$2.17(\pm0.23)\times10^{-3}$	8.55 ± 0.19	0.9725	8.65	8.12
ErHEDTA	$5.33(\pm0.11)\times10^{-4}$	8.46 ± 0.05	0.9914	8.63	8.07
TmHEDTA	$6.26(\pm0.03)\times10^{-4}$	8.24 ± 0.03	0.9978	8.66	8.03
YbHEDTA	$5.36(\pm0.12)\times10^{-4}$	8.18 ± 0.06	0.9978	8.56	8.00
LuHEDTA	$4.99(\pm0.19)\times10^{-4}$	8.46 ± 0.10	0.9169	8.64	7.98

[a] Ref.[21] [b] Ref.[22]

All fits are quite good, with R^2 values close to 1.00, except for NdHEDTA, HoHEDTA, and LuHEDTA. It is found that the pK_h values obtained by our present kinetic

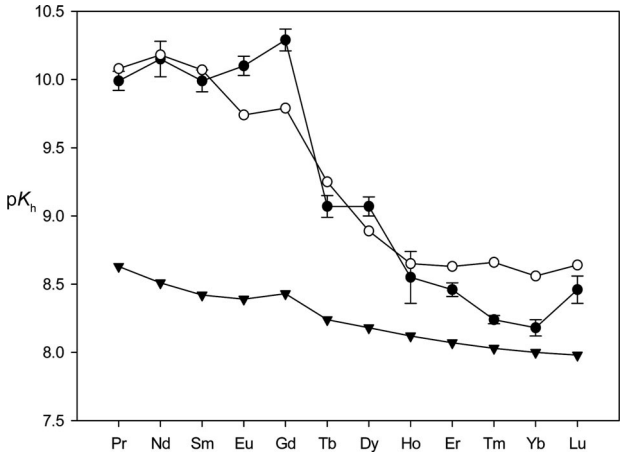

Figure 2. Plots of the pK_h values of LnHEDTA and Ln^{3+} ions: LnHEDTA, this work (●); LnHEDTA, ref.[21] (○); Ln^{3+}, ref.[22] (▼).

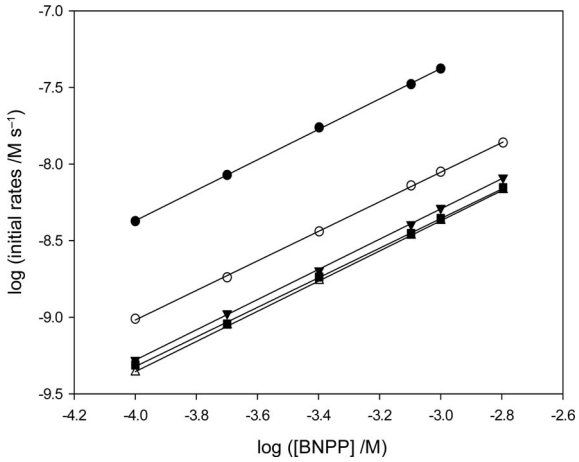

Figure 3. Plots of log (initial rates) vs. log[BNPP] for selected LnHEDTA complexes (Ln = Nd, ○; Eu, ●; Dy, ▼; Er, Δ; Yb, ■). [LnHEDTA] = 10 mM, [buffer] = 100 mM, [BNPP] = 0.1 mM to 1.6 mM, pH = 10.5 at 25 °C. The solid lines are the best linear least-squares fits ($R^2 \approx 1.0$).

method decrease with increasing atomic number of lanthanides and are consistent with those reported previously.[21] It is interesting to observe that, upon HEDTA complexation, the ΔpK_h values [ΔpK_h = pK_h(LnHEDTA) – pK_h(Ln^{3+})] decrease as the atomic number of lanthanides increases (Figure 2). The ionic radius of trivalent lanthanide ions decreases with increasing atomic number, and the charge density increases with increasing atomic number. From the variation of the ΔpK_h values, it is possible that upon HEDTA complexation, the effect that charge density exerts on the coordinated water molecules is less "tuned" for heavier lanthanide ions. The phenomenon of "gadolinium break" is also quite obvious.

The $k_{LnL(OH)}$ value increases from PrHEDTA to SmHEDTA, EuHEDTA, and GdHEDTA, and then decreases gradually to TbHEDTA and DyHEDTA. It increases again to HoHEDTA and then decreases at ErHEDTA to LuHEDTA. This will be discussed later.

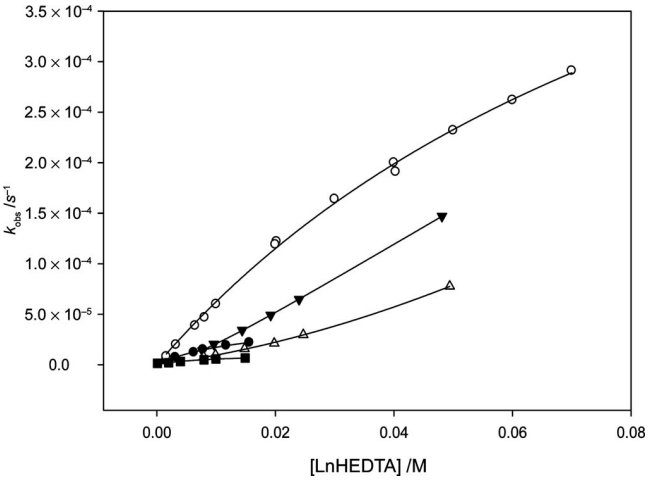

Figure 4. Selected plots of k_{obs} vs. [LnHEDTA]. [LnHEDTA] = 1.0–70 mM, [BNPP] = 0.1 mM, [buffer] = 100 mM, μ = 0.1 M at 25 °C. The solid lines are the best least-squares fits to Equation (2) except for Tb and Ho. ●, Nd; ○, Eu; ▼, Tb; Δ, Ho; ■, Yb.

Reactions of BNPP with LnHEDTA at pH 10.5

To understand the reactions of BNPP with LnHEDTA better, we determined the k_{obs} values at pH 10.5 as a function of [LnHEDTA]. We first determined the order of dependence of BNPP by varying [BNPP] from 0.1 mM to 1.6 mM while keeping [LnHEDTA] at 10.0 mM. Figure 3 shows the log (initial rates) vs. log[BNPP] plots for selected LnHEDTA (Ln = Nd, Eu, Dy, Er, Yb) complexes. The slopes and R^2 values of the linear least-squares regression analyses are all close to unity, indicating that the reactions with respect to BNPP are all first order (data not shown).

The observed k_{obs} values for the reactions of BNPP with LnHEDTA complexes at pH 10.5 as a function of [LnHEDTA] are listed in Table S2 (Supporting Information). Selected plots of k_{obs} values vs. [LnHEDTA] are shown in Figure 4.

From the data in Table S2 and Figure 4, it is observed that most of the k_{obs} values increase with [LnHEDTA], and saturation kinetic curves were obtained for all complexes except for HoHEDTA and TbHEDTA, for which more than first-order dependence curves were obtained. The data for DyHEDTA were limited because of its low solubility and could also be treated with a saturation reaction mechanism shown in Scheme 2.

$$\mathrm{LnHEDTA(OH)^- + BNPP} \overset{K}{<=>} \mathrm{LnHEDTA(OH)^-BNPP} \xrightarrow{k_1} \mathrm{Products}$$

$$k_{obs} = k_1K[\mathrm{LnHEDTA(OH)^-}]/(1 + K[\mathrm{LnHEDTA(OH)^-}]) \qquad (2)$$

Scheme 2.

Fitting the k_{obs} values to [LnHEDTA] in Equation (2), we obtain the equilibrium constants, K, and the rate constants, k_1 (Table 2). Note that the [LnHEDTA(OH)$^-$] value

is calculated by considering K_h, i.e. $[LnHEDTA(OH)^-] = [LnHEDTA]_T/(1 + [H^+]/K_h)$.

Table 2. The fitted k_1 and K values for BNPP reactions at various [LnHEDTA].

	k_1 /s^{-1}	K /M^{-1}	R^2
PrHEDTA	1.46×10^{-5}	146.8	0.9939
NdHEDTA	1.06×10^{-4}	15.5	0.9961
SmHEDTA	2.94×10^{-4}	12.1	0.9999
EuHEDTA	6.36×10^{-4}	10.2	0.9981
GdHEDTA	2.42×10^{-3}	2.01	0.9999
TbHEDTA	(2.71×10^{-3})[a]	–	1.000
DyHEDTA	3.75×10^{-5}	21.7	0.9998
HoHEDTA	(7.33×10^{-4})[a]	–	0.9999
ErHEDTA	1.12×10^{-5}	68.1	0.9987
TmHEDTA	2.37×10^{-5}	44.8	0.9988
YbHEDTA	3.69×10^{-5}	18.1	0.9937
LuHEDTA	1.34×10^{-5}	77.3	0.9956

[a] The rate constants for TbHEDTA and HoHEDTA (k_1, M^{-1} s^{-1}) were obtained by fitting the data to $k_{obs} = k_1[LnHEDTA] + k_2[LnHEDTA]^2$, i.e. Scheme 3. Note that the units for k_1 are different for Scheme 2 (s^{-1}) and for Scheme 3 (M^{-1} s^{-1}).

The k_1 values for TbHEDTA and HoHEDTA in Table 2 were obtained by fitting the corresponding data to a quadratic equation in the form $k_{obs} = k_1[LnHEDTA] + k_2[LnHEDTA]^2$ [Equation (3)], according to the mechanism shown in Scheme 3. The k_2 values were 7.77×10^{-3} M^{-2} s^{-1} and 1.61×10^{-2} M^{-2} s^{-1} for TbHEDTA and HoHEDTA, respectively. In general, the fitted k_1 values by [LnHEDTA]-dependence data at pH 10.5 (i.e. 1.1×10^{-5} to 2.7×10^{-3} M^{-1} s^{-1}) increase from PrHEDTA to GdHEDTA and TbHEDTA and then decrease as the atomic numbers of lanthanides increase. These values are similar to or greater than those of Ln^{3+} catalyzed BNPP hydrolysis reactions at pH 7.0 (i.e. 1.3×10^{-5} to 5.0×10^{-4} M^{-1} s^{-1}).[4]

$$LnHEDTA(OH)^- + BNPP \rightarrow Products \qquad k_1$$

$$2LnHEDTA(OH)^- + BNPP \rightarrow Products \qquad k_2$$

$$k_{obs} = k_1[LnHEDTA(OH)^-] + k_2[LnHEDTA(OH)^-]^2 \qquad (3)$$

Scheme 3.

The binding constant values, K, for the formation of LnHEDTA(OH)$^-$BNPP are in the range 2–147 M^{-1} and are, as expected, smaller than those of Ln^{3+}-BNPP,[4] which are in the order of 10^3 M^{-1}. A biphasic characteristic is shown: the value decreases from Pr to Nd, Sm, Eu, and Gd, then increases at Dy and Er, decreases again at Tm and Yb, and then increases at Lu (Figure 5). Our tentative explanation to account for the larger K values for the heavier lanthanide–HEDTA complexes is to attribute this behavior to their greater charge densities. For the lighter PrHEDTA complex, the number of inner-sphere coordinated water molecules is possibly 4, which is more than those of LnHEDTA (Ln = Nd, Eu, Gd) with 3 inner-sphere coordinated water molecules.[23,24] This leads to a larger K value because more coordinated sites and space are available for BNPP binding with less negative charge repulsion. The SmHEDTA(OH)$^-$, EuHEDTA(OH)$^-$, and GdHEDTA-(OH)$^-$ complexes have the lowest K values, leading to greater hydrolysis rates.

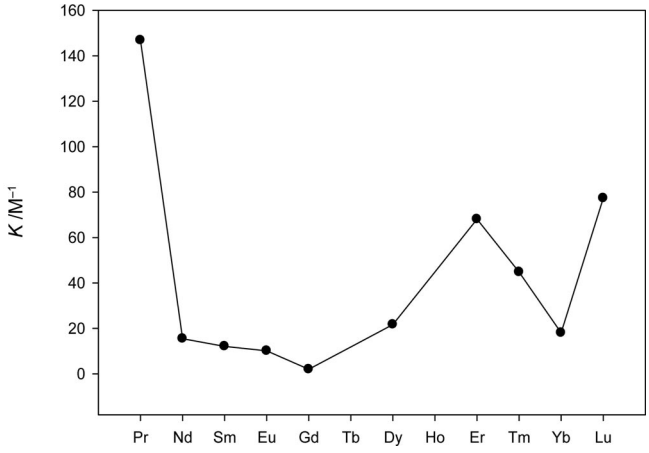

Figure 5. Plots of formation constants of LnHEDTA(OH)$^-$BNPP.

Reactions of BNPP with TbHEDTA and HoHEDTA at pH 10.5

For the pH-dependent BNPP hydrolysis studies, it was found that HoHEDTA has a poorer pK_h data fit with a relatively larger variation of the $k_{LnL(OH)}$ value (Table 1, Figure 2). For the [LnHEDTA]-dependent studies, both TbHEDTA and HoHEDTA data have greater than first-order dependence. Scheme 3 is one possible proposed mechanism (vide supra). Another more preferred, possible mechanism involving $\{LnHEDTA(OH)^-\}_2$ dimer formation is shown in Scheme 4.

$$LnHEDTA(H_2O) \; <=> \; LnHEDTA(OH)^- + H^+ \qquad K_h$$

$$2LnHEDTA(OH)^- \; <=> \; \{LnHEDTA(OH)^-\}_2 \qquad K_f$$

$$LnHEDTA(OH)^- + BNPP \rightarrow Products \qquad k_1$$

$$\{LnHEDTA(OH)^-\}_2 + BNPP \rightarrow Products \qquad k_2$$

$$Rate = k_1[LnHEDTA(OH)^-][BNPP] + k_2[\{LnHEDTA(OH)^-\}_2][BNPP]$$

$$Rate = k_1[LnHEDTA(OH)^-][BNPP] + k_2K_f[LnHEDTA(OH)^-]^2[BNPP]$$

$$k_{obs} = k_1[LnHEDTA(OH)^-] + k_2K_f[LnHEDTA(OH)^-]^2 \qquad (4)$$

Scheme 4.

Fitting the rate data to Scheme 4 [Equation (4)] model and using pK_h values 9.07 and 8.55 for TbHEDTA and HoHEDTA, respectively, gives the equilibrium and rate constants as follows: K_f = 112 M^{-1} (TbHEDTA), 0.265 M^{-1} (HoHEDTA); $k_1 = 7.72 \times 10^{-12}$ M^{-1} s^{-1} (TbHEDTA), 8.06×10^{-4} M^{-1} s^{-1} (HoHEDTA); $k_2 = 8.39 \times 10^{-3}$ M^{-1} s^{-1} (TbHEDTA), 6.50×10^{-2} M^{-1} s^{-1} (HoHEDTA).

$$[LnHEDTA]_T = [LnHEDTA(H_2O)] + [LnHEDTA(OH)^-] + 2[\{LnHEDTA(OH)^-\}_2]$$

$$= [LnHEDTA(OH)^-][H^+]/K_h + [LnHEDTA(OH)^-] + 2K_f[LnHEDTA(OH)^-]^2$$

$$2K_f[LnHEDTA(OH)^-]^2 + ([H^+]/K_h + 1)[LnHEDTA(OH)^-] - [LnHEDTA]_T = 0$$

$$[LnHEDTA(OH)^-] = \{-([H^+]/K_h + 1) + (\{[H^+]/K_h + 1\}^2 + 8K_f[LnHEDTA]_T)^{1/2}\}/4K_f$$

The quantity [LnHEDTA(OH)$^-$], could be easily calculated by considering the mass balance and equilibrium expressions as follows:

Considering the mechanisms shown in Scheme 3 and Scheme 4 and the resulting fitted data, it can be concluded that (1) the dimerization constant is larger for TbHEDTA, and (2) the dimer is more reactive for HoHEDTA than TbHEDTA toward BNPP hydrolysis. However, even if the dinuclear species are more reactive, the reactivities for LnHEDTA (Ln = Tb, Ho) are still lower than those of LnHEDTA (Ln = Sm, Eu, and Gd) in the present [LnHEDTA] range studied. Only, at greater [LnHEDTA], the TbHEDTA complex might be more reactive than EuHEDTA. It should be noted that laser-excited luminescence studies revealed that the number of inner-sphere coordinated water molecules is one per TbHEDTA molecule at pH > 10, indicating that the TbHEDTA complex is likely to form a dinuclear, OH^- bridged species.[25] Several previous publications also pointed out that TbHEDTA complexes form a higher order of oligomers at pH > 10.[26,27] The exact nature of lanthanide hydroxide/oxide oligomer formation is complex. It should be related to the bond length of Ln–L and bond angle of L–Ln–L (L = OH^- and O^{2-}) and may vary when they are chelated by multidentate ligands, which remains to be delineated in the future.

HPLC Analysis

Figure S1 shows the chromatograms of the reaction between BNPP and EuHEDTA at pH 10.5. It is observed that the concentration of BNPP decreases with time and the concentrations of NP and NPP increase with time, as expected. Unlike the same reaction at pH 11.0, where a small amount of NPP was further hydrolyzed to NP,[17] BNPP is only hydrolyzed to NPP and NP and no further hydrolysis is observed for NPP at pH 10.5. After converting the peak areas of BNPP, NPP, and NP to concentrations from previously constructed calibration curves, we obtain the concentration vs. time plots as shown in Figure 6. Fitting the curves in Figure 6 for BNPP {to exponential decay to a minimum, $[LnL]_t = a\exp(-k_{obs}t)$, where $[LnL]_t$ is the [LnL] at time t} and NP {to exponential growth to a maximum, $[LnL]_t = a(1 - \exp\{-k_{obs}t\})$}, we obtain the observed rate constants (k_{obs}) and initial concentrations for BNPP (a), and they are listed in Table 3. It is found that the decay rate constant of BNPP and the growth rate constant of NP are, as expected, very similar. However, for NPP, the apparent concentrations are all higher than those calculated from calibration curve data. One possibility is that the NPP retention time is very close to that of the solvent peak, t_o, and therefore quantitation is subject to larger error. Another possibility is that the reaction is actually a transesterification reaction in which the NPP group is transferred from BNPP to the coordinated *N*-hydroxyethyl group with a greater molar absorptivity than that of the free NPP. There are several similar previous examples in the literature.[8–9] Fitting of the [EuHEDTA-NPP] vs. time data to the exponential growth to a maximum curve gives a rate constant much lower than that of NP and BNPP. This is mainly due to the fact that the retention time of the EuHEDTA-NPP peak is very close to that of the solvent peak, making the determination of concentration more difficult and with larger error.

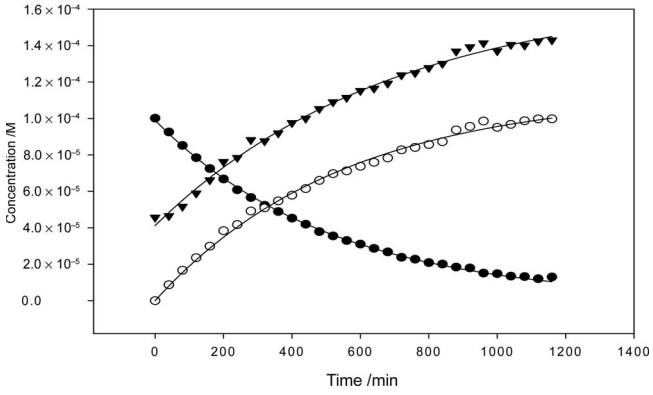

Figure 6. The concentration vs. time plots for the reaction of EuHEDTA with BNPP at pH 10.5 from HPLC analysis data. The solid lines are the best least-squares fits to the corresponding exponential curves. ●, BNPP; ○, NP; ▼, NPP. [EuHEDTA] = 10 mM, [BNPP] = 0.10 mM, [buffer] = 100 mM, μ = 0.1 M.

Table 3. Observed rate constants for BNPP, NP, and NPP at pH 10.5 from HPLC analysis. [EuHEDTA] = 10 mM, [BNPP] = 0.10 mM, [buffer] = 100 mM, μ = 0.1 M.

	k_{obs} /s^{-1}	a (init. conc.) /M
BNPP decay rate constant	$3.23(\pm0.01)\times10^{-5}$	0.99 ± 0.01
NP growth rate constant	$3.03(\pm0.06)\times10^{-5}$	1.14 ± 0.02
NPP growth rate constant	$2.40(\pm0.10)\times10^{-5}$	1.28 ± 0.04

The observed rate constants could also be estimated from initial rate data. However, there are only limited data points from HPLC studies and a rate constant of $3.13(\pm0.01)\times10^{-5}$ s^{-1} is obtained from the first three [BNPP] data points, which cover approximately 15% of the reaction. This value is similar to that obtained from the pH-dependent study but slightly lower than that obtained from the [LnL]-dependent study. The rate constants obtained from the initial rate data are also similar to those obtained from the integral rate data within experimental error.

ESI-MS and Structural Studies

The ESI(–)-MS spectrum of EuHEDTA + BNPP reaction products at pH 10.5 is shown in Figure 7.

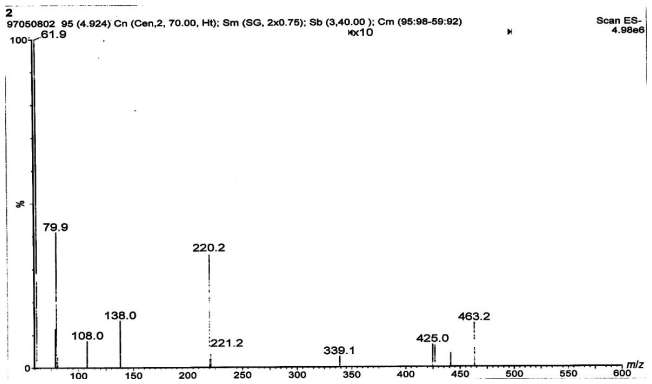

Figure 7. ESI(–)-MS spectrum of the reaction of BNPP with EuHEDTA at pH 10.5 (CAPS buffer). m/z = 61.9, (NO_3^-); 79.9, ($NO_3^-{\cdot}H_2O$); 108.0, (NPP, $C_6H_4NO_6P)^{2-}$; 138.0, (NP, $C_6H_4NO_3)^-$; 220.2, 221.2 (CAPS, $C_9H_{18}NO_3S)^-$; 339.1, (BNPP, $C_{12}H_8N_2O_8P)^-$; 425.0, 427.0 ($Eu^{151,153}HEDTA)^-$; 441.6, (CAPS dimer + $H^+)^-$; 463.2, (CAPS dimer + $Na^+)^-$.

It is clear that the two peaks at m/z = 425 and 427 are from the isotopic $Eu^{151,153}HEDTA^-$. However, no peaks are shown for EuHEDTA-NPP^- at m/z = 643 and 645. Instead, a peak at m/z = 108 is present for the free NPP^{2-} anion. This indicates that the reaction between EuHEDTA and BNPP at pH 10.5 is a simple hydrolysis but not a transesterification reaction. This is quite different from the reaction of $EuTHED^{3+}$ with m^7GpppG, in which a transesterification reaction takes place.[8]

To further understand the possible structure–reactivity relationship, it is important to compare the structures of the two complexes, EuHEDTA and $EuTHED^{3+}$. Unfortunately, neither of the two crystal structures has been reported. However, the analogous structures of $EuEDTA^-$ and $Eu(s\text{-}THP)^{3+}$ [s-THP = 1,4,7,10-tetrakis(2-hydroxypropyl)-1,4,7,10-tetraazacyclododecane] are known.[28,29] From these structures, the estimated distances of the coordinated hydroxyethyl oxygen atom to that of the nearest inner-sphere coordinated H_2O oxygen is roughly 2.97 and 2.76 Å for EuHEDTA and $EuTHED^{3+}$, respectively. Thus, it could be rationalized that when BNPP replaces an apical inner-sphere coordinated water molecule on $EuTHED^{3+}$, the nucleophilic attack could be taking place more easily between the coordinated ethyl oxide group and the BNPP anion. On the other hand, the distance is too far between the coordinated ethyl oxide group and BNPP on EuHEDTA for the nucleophilic attack. Instead, hydrolysis is likely to occur by proton transfer from one inner-sphere coordinated water molecule to the deprotonated ethyl oxide group followed by a nucleophilic attack of the resulting hydroxide ion on the bonded BNPP anion.

Conclusion

The implications of this study are at least threefold: One is that complexation of trivalent lanthanide ions leads to varying degrees of modification of their chemical and perhaps physical properties including their inner-sphere coordinated water hydrolysis constants, hydroxido-/oxido-bridged oligomer formation, and various catalytic reactivities. The second is that for the (enzymatic) lanthanide active sites, small structural differences may result in different reaction mechanisms and products. The third is that by subtle ligand design, it may be possible to affect the reactivities of trivalent lanthanide complexes as artificial nucleases and ribonucleases by taking advantage of the variations in their charge density, size and number, and the spatial arrangements of their inner-sphere coordinated water molecules.

Experimental Section

Materials and Standard Solutions

Analytical reagent-grade chemicals and buffers, unless otherwise stated, were purchased from Sigma (St. Louis, MO, USA), Aldrich (Milwaukee, Wl, USA), or Merck (Darmstadt, Germany) and were used as received without further purification. Disodium ethylenediaminetetraacetic acid (EDTA) and *N*-hydroxyethyl(ethylenediamine)-*N*,*N*′,*N*′-triacetic acid (HEDTA) were purchased from Aldrich. BNPP [sodium bis(*p*-nitrophenyl)phosphate] was purchased from SIGMA with free *p*-nitrophenol impurity < 0.05%. Carbonate-free deionized water was used for the preparation of all solutions.

The concentration of HEDTA stock solution (ca. 0.1 M) was determined by acid–base titration against a standard tetramethylammonium hydroxide solution (0.1 M).[15] The concentrations of the lanthanide nitrate stock solutions were ca. 0.1 M and they were standardized by EDTA titration with xylenol orange as indicator. The tetramethylammonium hydroxide solution (0.1 M) was prepared by diluting a 20% $(CH_3)_4NOH$/methanol solution obtained from Aldrich (carbonate-free). The aqueous $(CH_3)_4NOH$ solution was standardized by using reagent-grade potassium hydrogen phthalate. A HCl solution (0.1 M) was prepared by diluting reagent-grade HCl to 1.0 M, then diluting the 1 M solution to 0.1 M. This solution was standardized by using the standard $(CH_3)_4NOH$ solution. A stock solution of tetramethylammonium chloride (Aldrich) (1.0 M) was prepared and diluted to 0.1 M for each titration to maintain a constant ionic strength (0.1 M).

Kinetic Measurements: All lanthanide–HEDTA complex solutions were freshly prepared by mixing solutions of the metal salt and the ligand in a molar ratio of 1.00:1.02. The pH of each solution was adjusted to 6.0–6.5 by adding the appropriate amount of $(CH_3)_4NOH$ solution. To each solution was then added the BNPP solution, and the final pH was adjusted by adding the appropriate amount of buffer stock solution. The solutions were used within 30 min after preparation. MPS (3-Morpholinopropanesulfonic acid, pK_a = 7.2), TAPS {3-[tris(hydroxymethyl)methylamino]-1-propanesulfonic acid, pK_a = 8.4}, CHES (2-[*N*-cyclohexylamino]-ethanesulfonic acid, pK_a = 9.3), CAPS (3-[cyclohexylamino]-1-propanesulfonic acid, pK_a = 10.4), and CABS (4-[cyclohexylamino]-1-butanesulfonic acid, pK_a = 10.7) were used to prepare buffer solutions with the desired pH. The final BNPP concentration was kept at 0.10 mM, and the lanthanide–HEDTA complex concentrations were 1.0 mM or greater to fulfill pseudo-first-order reaction conditions. The ionic strength was adjusted to 0.1 M with $(CH_3)_4NCl$. A HP 8453 UV/Vis spectrophotometer was used to measure the increase in absorption with time at 400 nm due to the formation of the nitrophenolate ion after the hydrolysis reaction of BNPP.[16] The observed rate constants were calculated by using the initial rate data. Most of the experiments were repeated twice or three

times and the average values were used. Sigma plot was used for curve fitting. The relative standard deviations were ≤ 15%.

HPLC Analysis: HPLC analyses of the reaction between EuHEDTA and BNPP at pH 10.5 were performed with a Waters Alliance® 2695HPLC system by using a Waters 2487 UV/Vis detector and a Waters Empower software. The reaction conditions were: [EuHEDTA] = 10 mM, [BNPP] = 0.10 mM, [buffer] = 100 mM, μ = 0.1 M, pH 10.5. Aliquots of the reaction solution were injected into the HPLC system and analyzed with a mobile phase containing 60% HPLC grade methanol and 40% 50 mM NaH_2PO_4/Na_2HPO_4 solution at pH 7.0. A C-18 column (Symmetry ® C18, 5 μm, 4.6 mm × 250 mm) was used as the stationary phase. Standard samples of 4-nitrophenolate (NP), 4-nitrophenyl phosphate (NPP), and BNPP were also injected for peak identification. Other parameters for the analyses were: flow rate = 0.5 mL min^{-1}, volume per injection = 10 μL, run time = 20 min, detection wavelength = 317 nm.

ESI Mass Spectrometry: Mass spectra were obtained with a triple quadrupole liquid chromatograph tandem mass spectrometer (Waters, Quattro Micro). The ESI condition was used for the negative mode: the syringe pump flow was set to 10.0 μL min^{-1}. The capillary energy was 2.60 kV. The cone gas flow was 503 L h^{-1}, and the energy was 30 V. The temperatures of the source and desolvation were 100 and 200 °C, respectively.

Supporting Information (see also the footnote on the first page of this article): Observed BNPP hydrolysis reaction rate constants (k_{obs}) calculated from the measured initial rate data at various solution pH values in the presence of 10 mM LnHEDTA, k_{obs} values for the reactions of BNPP with LnHEDTA complexes at pH 10.5 as a function of [LnHEDTA], and chromatograms of the reaction between BNPP and EuHEDTA at pH 10.5.

Acknowledgments

The authors wish to thank the National Science Council of the Republic of China (Taiwan) for financial support (grant number NSC-95-2113-M-009-025) of this work. A grant from the National Science Council/Atomic Energy Council (grant number 96-NU-7-009-003) is also acknowledged. We thank Mr. Kuan-Yu Liu for help in crystal structure literature search and initial molecular modeling studies.

[1] J. K. Bashkin, B. N. Trawick, A. T. Daniher, *Chem. Rev.* **1998**, *98*, 939–960.
[2] M. Oivanen, S. Kuusela, H. Lonnberg, *Chem. Rev.* **1998**, *98*, 961–990.
[3] N. H. Williams, B. Takasaki, M. Well, J. Chin, *Acc. Chem. Res.* **1999**, *32*, 485–493.
[4] A. Roigk, R. Hettich, H.-J. Schneider, *Inorg. Chem.* **1998**, *37*, 751–756.
[5] S. Amin, J. R. Morrow, C. H. Lake, M. R. Churchill, *Angew. Chem. Int. Ed. Engl.* **1994**, *33*, 773–775.
[6] B. K. Takasaki, J. Chin, *J. Am. Chem. Soc.* **1994**, *116*, 1121–1122.
[7] P. Hurst, B. K. Takasaki, J. Chin, *J. Am. Chem. Soc.* **1996**, *118*, 9982–9983.
[8] B. F. Baker, H. Khalili, N. Wei, J. R. Morrow, *J. Am. Chem. Soc.* **1997**, *119*, 8749–8755.
[9] I. L. Chappell, D. A. Voss Jr, W. D. Horrocks Jr, J. R. Morrow, *Inorg. Chem.* **1998**, *37*, 3989–3998.
[10] D. M. Epstein, L. L. Chappell, H. Khalili, R. M. Supkowski, W. D. Horrocks Jr, J. R. Morrow, *Inorg. Chem.* **2000**, *39*, 2130–2134.
[11] P. Gómez-Tagle, A. K. Yatsimirsky, *Inorg. Chem.* **2001**, *40*, 3786–3796.
[12] P. Gómez-Tagle, A. K. Yatsimirsky, *J. Chem. Soc., Dalton Trans.* **2001**, 2663–2670.
[13] A. Aguilar-Perez, P. Gomez-Tagle, E. Collado-Fregoso, A. K. Yatsimirsky, *Inorg. Chem.* **2006**, *45*,9502–9517.
[14] E. R. Farquhar, J. P. Richard, J. R. Morrow, *Inorg. Chem.* **2007**, *46*, 7169–7177.
[15] C. A. Chang, F. K. Shieh, Y.-L. Liu, Y.-H. Chen, H.-Y. Chen, C.-Y. Chen, *J. Chem. Soc., Dalton Trans.* **1998**, 3243–3248.
[16] C. A. Chang, B. H. Wu, P. Y. Kuan, *Inorg. Chem.* **2005**, *44*, 6646–6654.
[17] C. A. Chang, et al., unpublished results.
[18] C. C. Fuller, D. K. Molzahn, R. A. Jacobson, *Inorg. Chem.* **1978**, *17*, 2138–2143.
[19] M. Komiyama, T. Shiiba, T. Kodama, N. Takeda, J. Sumaoka, M. Yashiro, *Chem. Lett.* **1994**, 1025–1028.
[20] M. Komiyama, N. Takeda, Y. Takahashi, H. Uchida, T. Shiiba, T. Kodama, M. Yashiro, *J. Chem. Soc. Perkin Trans. 2* **1995**, 269–274.
[21] A. K. Gupta, J. E. Powell, *Inorg. Chem.* **1962**, *1*, 955–966.
[22] R. M. Smith, A. E. Martell, *Critical Stability Constants*, **1974**–**1989**.
[23] T. Kimura, Y. Kato, *J. Alloys Compd.* **1998**, *271*, 867–871.
[24] T. Kimura, Y. Kato, *J. Alloys Compd.* **1998**, *275*, 806–810.
[25] C. A. Chang, H. B. Brittain, J. Telser, M. F. Tweedle, *Inorg. Chem.* **1990**, *29*, 4468–4473.
[26] L. Spaulding, H. G. Brittain, *Inorg. Chem.* **1983**, *22*, 3486–3488.
[27] G. Hernandez, H. G. Brittain, M. F. Tweedle, R. G. Bryant, *Inorg. Chem.* **1990**, *29*, 985–988.
[28] J. Wong, X. D. Zhang, W. G. Jia, Y. Zhang, Z. R. Liu, *Russ. Koord. Khim.* **2004**, *30*, 141.
[29] K. O. A. Chin, J. R. Morrow, C. H. Lake, M. R. Churchill, *Inorg. Chem.* **1994**, *33*, 656–664.

Received: October 22, 2008
Published Online: February 5, 2009

